Int J Clin Exp Med 2018;11(5):4639-4646
www.ijcem.com /ISSN:1940-5901/IJCEM0074544

Original Article

Expression and function of IgSF21 in amacrine cells in a diabetic retinopathy model

Xiaohui Lin[1], Jihong Wang[2], Yingying Li[1], Xiaocheng Ma[1], Zhen Li[1], Yihui Zhang[1]

[1]Department of Ophthalmology, The Inner Mongolia Autonomous Region People's Hospital, Hohhot 010017, Inner Mongolia Autonomous Region, China; [2]The Second Department of Hand and Foot Microsurgery, The Second Affiliated Hospital of Inner Mongolia Medical University, Hohhot, Inner Mongolia Autonomous Region, China

Received February 13, 2018; Accepted March 24, 2018; Epub May 15, 2018; Published May 30, 2018

Abstract: Objective: Our aim was to study the role and mechanism of immunoglobulin superfamily member 21 (IgSF21) expression in diabetic retinopathy (DR). Methods: Sprague-Dawley rats were injected with streptozotocin to create the diabetic model. Rats with diabetes were divided into three groups based on their feeding periods: group A (fed for 8 weeks), group B (fed for 12 weeks), and group C (fed for 16 weeks). Levels of IgSF21 mRNA and protein in rat retinal tissues from these groups were measured by quantitative reverse transcription PCR and Western blot. Amacrine cells were isolated from rat eyeballs and miniature inhibitory postsynaptic currents (mIPSCs) were detected using patch clamp technique. Plasmid expressing IgSF21 was constructed and transfected into amacrine cells. Co-localization of IgSF21 and neurexin2α and the interaction between these two proteins were analyzed through immunofluorescence (IF) and co-immunoprecipitation (co-IP). The impact of IgSF21 overexpression on mIPSCs in amacrine cells was investigated. Results: As compared with control group, expressions of IgSF21 mRNA in rats with DR in groups A, B and C, as well as expressions of IgSF21 protein in groups B and C were all reduced. Furthermore, the frequencies of mIPSCs in gamma-aminobutyric acid-ergic (GABAergic) amacrine cells in all three groups also decreased, with reduction in group C the greatest (all $P<0.05$). Through IF assay, it was found that IgSF21 and neurexin2α proteins were co-localized. The co-IP was conducted and direct interaction between these two proteins was detected. Using a patch clamp technique, it was also found that both frequency and current amplitude of mIPSCs rose when IgSF21 was overexpressed ($P<0.05$). Conclusion: IgSF21 can act on neurexin2α directly and affect the function of GABAergic amacrine cells while reduction in IgSF21 levels may accelerate progression of DR.

Keywords: Immunoglobulin superfamily member 21, diabetic retinopathy, mechanism research

Introduction

Diabetic retinopathy (DR) is a common complication in patients with diabetes which, in some cases, could even cause blindness. Incidence of DR rises as the course of diabetes prolongs [1]. One of the main manifestations of DR is increase in retinal microvascular permeability which can lead to capillary basal lamina thickening and endothelial cell division abnormality, causing loss of transport function in capillaries. The pathogenesis of DR is quite complicated. Some scholars believe that the imbalance between generation and degradation of free radicals within the body can increase the level of reactive oxygen species, disrupt relevant signaling pathways, and as a result, affect gene transcription of key proteins in the nucleus [2, 3]. Shah et al. reported that high blood sugar levels in patients with diabetes can cause non-enzymatic glycosylation in capillaries, thus bringing about accumulation of advanced glycation end products in retinal capillaries which disrupts the physiological function of the retina, increases oxidative stress in relevant cells and tissues, and activates caspase-3 to promote apoptosis of capillary cells [4]. Modern medical research has found that amacrine cells, bipolar cells, and ganglion cells, as relatively simple parts in central nervous system, can form synapses. Among them, gamma-aminobutyric acid-ergic (GABAergic) amacrine cells, a type of interneuron that can produce inhibitory signals, play a key role in the formation of vision. Its neurotransmission can be affected by high blood sugar content which may lead to aggrava-

tion of DR and even cause blindness in patients [5, 6]. The excitability of amacrine cells can be expressed through miniature inhibitory postsynaptic currents (mIPSCs). Neurexin2α is an important protein that participates in the release of neurotransmitters from presynaptic membranes regulated by neurons. It can stimulate mIPSCs in neurons and, therefore, activate neurotransmission [7]. However, it is still unclear which component regulates neurexin2α. Proteins in the immunoglobulin superfamily (IgSF) have structures similar to that of an antibody, which can regulate signaling pathways, adjust immune function, and mediate adhesion of lymphocytes to target cells. Immunoglobulin superfamily member 21 (IgSF21) belongs to this group. It can promote the formation of synapses and helps with maintenance of neuronal function [8]. At present, mechanisms of IgSF21 and neurexin2α are still unclear. Therefore, our present study investigated expression of IgSF21 in amacrine cells in DR rat model as well as interaction between IgSF21 and neurexin2α, in an effort to obtain some useful information for treating this disease.

Materials and methods

Animal subjects

A total of 80 two-month-old male Sprague-Dawley rats were chosen as subjects (clean grade, 170 ± 25 g, purchased from Anpel Laboratory Technologies (Shanghai) Inc., approval No. SYXK (Hu) 2005-0001). Ten rats were fed with a normal diet as control whereas the remaining 70 rats were used to create a diabetic rat model by receiving a single-dose intraperitoneal injection of 2% streptozotocin (STZ, diluted in citrate buffer solution, pH=4.5, dosage: 50 mg/kg) after 3 days of adaptive feeding. Rats in the control group were injected with the same volume of normal saline. Blood sugar levels were tested after two days. The model was created successfully if the blood sugar content was above 16.9 mmol/L. After that, rats with DR (symptoms included fundus hemorrhage and edema) were picked at 8^{th}, 12^{th} and 16^{th} week, respectively, and were assigned into group A, B and C (ten rats in each group).

Main reagents and instruments

Main reagents, instruments, and supplier information were as follows: STZ (Merck, Germany), rabbit anti-mouse IgSF21 and goat anti-mouse neurexin2α monoclonal antibody (Abcam, UK), enhanced chemiluminescence (ECL) reagent (Beyotime Biotechnology), RT-PCR kit, bicinchoninic acid (BCA) protein quantification kit and TRIzol kit (Tiangen Biotech (Beijing) Co., Ltd), fetal bovine serum (FBS, Hyclone, US), ELISA kit and immunohistochemistry (IHC) kit (Shanghai Yanjin Biotech Co., Ltd), versatile Arktik PCR device (Thermo, USA), electrophoresis instrument (model DYY-12, Beijing Liuyi Biotech Co., Ltd), inverted microscope (model IX51, Olympus, Japan), patch-clamp system (Nanion, Germany), confocal fluorescence microscope (3I, USA), and pCMV-Myc plasmid and competent Escherichia coli (E.coli) DH5α (kept in our lab).

Methods

Isolation and culture of amacrine cells: Normal rats and rats with DR were sacrificed by cervical dislocation after anesthesia. The eyeballs were taken out and fasciae around the eyes were removed. Under the dissecting microscope, crystalline lenses were resected and retinal neuroepithelial layers were stripped. Samples were placed in D-Hank's solution containing 12 mM HEPES and then put in incubator for trypsinization at 37°C for 10 minutes. FBS was then added at 0.5 mL to cease trypsinization. Supernatant was discarded after centrifugation and Dulbecco's modified eagle medium (DMEM) was added to resuspend retinal cells. Next, some retinal cells were moved to culture plates containing DMEM, with 5-bromo-2'-deoxyuridine added in the meantime to inhibit growth of non-neural cells. Samples were incubated at 37°C in an atmosphere of 5% CO_2 for 72 hours and were later placed under phase contrast microscope for observing growth of GABAergic amacrine cells. Cell somata were generally over 10 μm in diameter with many slender processes, which intersected with those in adjacent cells to form a network [9].

Patch clamp technique: The patch clamp technique was applied for measuring mIPSCs in neurons and to observe excitability. After culture, samples were washed in Tyrode's solution twice. The electrolyte solution was added to set electrical resistance at 4-5 MQ. The electrode tip was adjusted to make sure that it was in contact with the surface of GABAergic amacrine cell and created high-resistance seal. Voltage

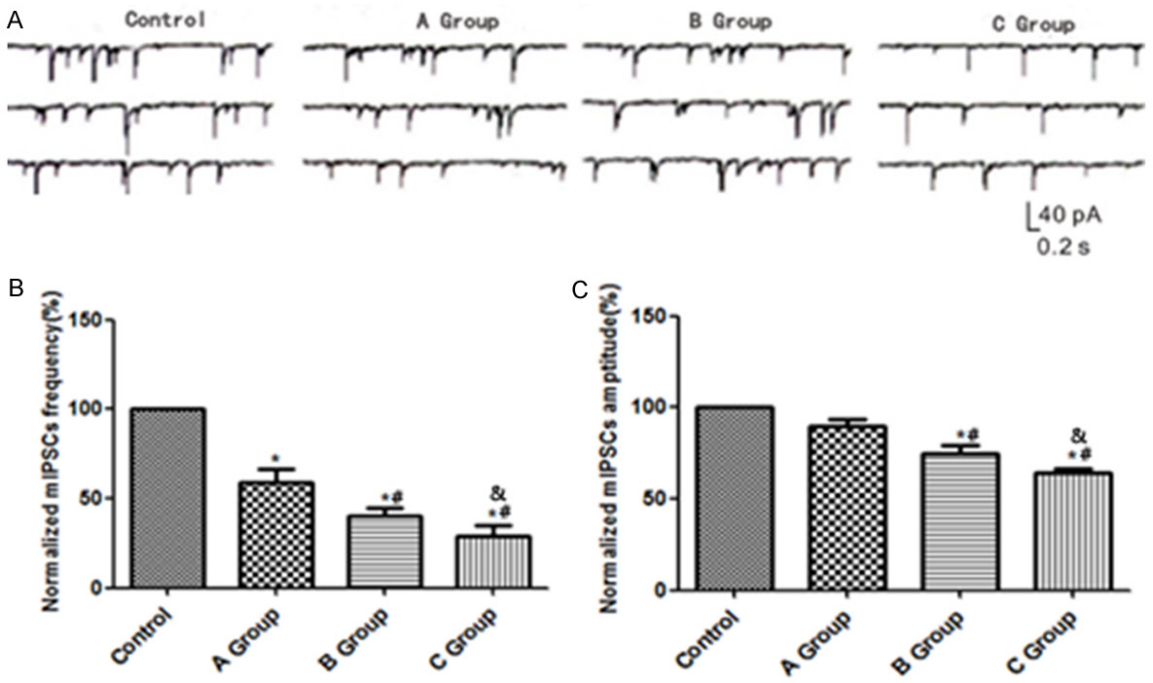

Figure 1. Changes in mIPSCs in GABAergic amacrine cells in rats with DR. A: Levels of mIPSCs measured by patch clamp technique in different groups; B: Histogram of mIPSCs frequencies in different groups; C: Histogram of current amplitudes of mIPSCS in different groups; *P<0.05 vs. control group, #P<0.05 vs. group A, &P<0.05 vs. group B. mIPCs, miniature inhibitory postsynaptic currents; GABAergic, gamma-aminobutyric acid-ergic; DR, diabetic retinopathy.

clamp was used to set voltage at -70 mV. The whole cell membrane current and fast capacitance compensation were recorded. Sampling and filter frequencies in analogue signal were set at 5 kHz and 1 kHz, respectively. All experiments were conducted at room temperature.

Detection of expression of IgSF21 mRNA by PCR: Fifty grams of retinal tissues were grounded in liquid nitrogen. Total RNA was extracted by TRIzol and checked for quality. After reverse transcription, samples were kept at -20°C. The level of IgSF21 mRNA was detected by SYBR Green quantitative fluorescence PCR. Gene for glyceraldehyde-3-phosphate dehydrogenase (GAPDH) was used as internal control and the primer was designed by Primer 5.0. The IgSF21 forward primer was 5'-CTAAGCTCCAGCTACTGC-3', while the reverse primer was 5'-CATGACTGCATAACGCTGAC-3'. GAPDH forward primer was 5'-CATACCATTGACTACACTGAC-3', and the reverse primer was 5'-CATCAGACCTACTACGACTC-3'. PCR running parameters were set as follows: 94°C 6 min, 94°C 20 s, 56°C 25 s and 72°C 40 s for 32 cycles, followed by 72°C 3 min at the end. Each reaction was done in triplicate. Relative gene expression of IgSF21 was calculated through $2^{-\Delta\Delta Ct}$ method.

Western blot: Retinal tissue (80 mg) was taken and added with 2 mL tissue lysate for protein extraction. Protein concentration was measured by BCA method. Protein samples were loaded into wells (25 μg per well) and separated by 12% SDS-PAGE. Afterward, proteins were transferred from gel to polyvinylidene fluoride membrane by tankblot. The membrane was then blocked with tris buffered saline with tween 20 (TBST) containing 5% skim milk powder for 30 minutes. Goat anti-mouse IgSF21 primary antibody was then added and the sample was incubated at 4°C for 8 hours, followed by the addition of secondary antibody conjugated to horseradish peroxidase (HRP) and a 2-hour incubation at room temperature. Samples were washed in TBST solution three times (5 min/per wash) and treated with ECL. After being photographed, the relative level of protein expression was analyzed with Gel Pro software.

Construction of eukaryotic expression plasmids pCMV-Myc-IgSF21 and pCMV-HA-neurexin2α:

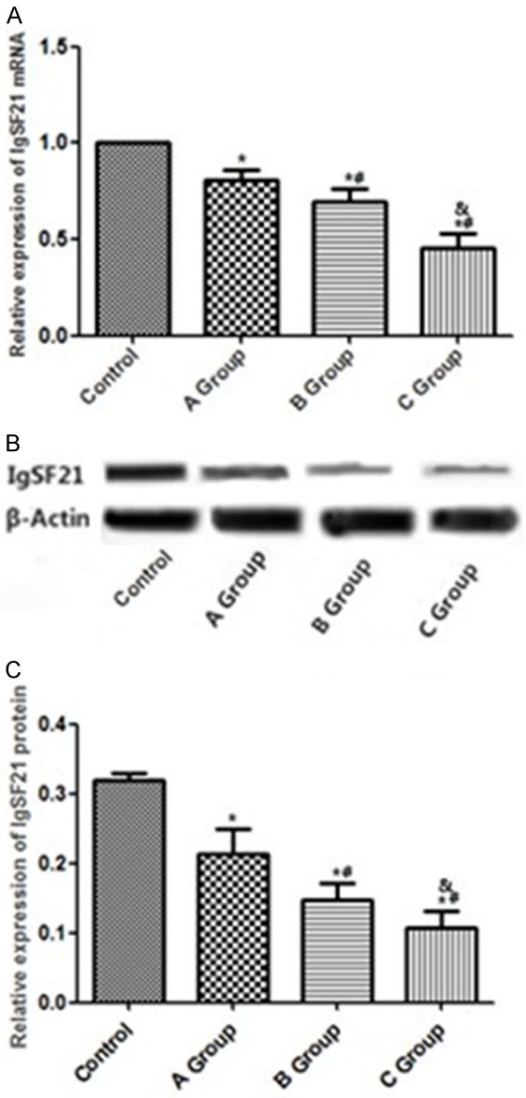

Figure 2. Changes in IgSF21 expression level in rats with DR. A: Levels of IgSF21 mRNA expression in different groups; B: Levels of IgSF21 protein expressions in different groups; C: Histogram regarding levels of IgSF21 protein expression in different groups; *P<0.05 vs. control, #P<0.05 vs. group A, &P<0.05 vs. group B. IgSF21, immunoglobulin superfamily member 21; DR, diabetic retinopathy.

Amacrine cells were lysed by TRIzol reagent and total RNA was extracted for reverse transcription after quality check. Gene primers for IgSF21 and neurexin2α were designed by Prime 5.0. Meanwhile, cutting sites for restriction enzymes, BamH1 and EcoR1, were created. The IgSF21 forward primer was 5'-CGATCAGTCGCCATGCAT-3', while the reverse primer was 5'-GTTCAGACGTACTGC-3'; the neurexin2α forward primer was 5'-CAGTCGGATCACTCAGC-3', and the reverse primer was 5'-CTGGACTACGTCACTGCAC-3'. After PCR reaction, the products were purified and collected. The amplified products, pCMV-Myc vector, and pCMV-HA vector were cut with restriction enzymes, BamH1 and EcoR1, and were treated with T4 ligase after purification. They were then transfected into competent E.coli and monoclonal bacteria were selected for culture. Target plasmids were then extracted, cut by enzyme, and verified by sequencing.

Immunofluorescence (IF) co-localization: GABAergic amacrine cells in logarithmic phase were selected. DMEM was renewed one day before transfection and cell density was controlled at $5*10^5$/mL. Cells were placed in a 12-well culture plate (0.5 mL per well). Transfection of pCMV-Myc-IgSF21 was performed according to the Lipofectamine-2000 instruction manual. Samples were incubated at 37°C for 72 hours in an atmosphere of 5% CO_2, followed by centrifugation at 1,500 rpm for 10 minutes, and washed in phosphate-buffered saline (PBS) three times. Some cell precipitations were taken and spread evenly over cover slips, which were then fixed by 4% formaldehyde for 20 minutes after getting briefly drying and were washed again in PBS three times. In order to increase membrane permeability, 0.1% Triton was added to cover the cells for 15 minutes. After being blocked for 30 minutes in 10% goat serum, rabbit anti-mouse IgSF21 antibody (1:500) and goat anti-mouse neurexin2α antibody were added into the sample for a 6-hour incubation. Afterward, goat anti-mouse secondary antibody (1:500) labeled with fluorescein isothiocyanate (FITC) and rabbit anti-goat secondary antibody (1:500) labeled with tetramethylrhodamine (TRITC) were added. Samples were then incubated for another two hours before being stained in 4', 6-diamidino-2-phenylindole (DAPI) solution for 8 minutes. Next, samples were washed in PBS once and incubated at 37°C for one hour before being washed again in PBS three times. Then, samples were fixed in 70% glycerin and observed under laser scanning confocal microscope.

Co-immunoprecipitation (co-IP): Amacrine cells from normal rats were cultured for 24 hours. When cell fusion reached around 60-80%, transfection of eukaryotic expression plasmids pCMV-Myc-IgSF21 and pCMV-HA-neurexin2α was conducted. Transfected amacrine cells were incubated at 37°C for 24 hours, followed

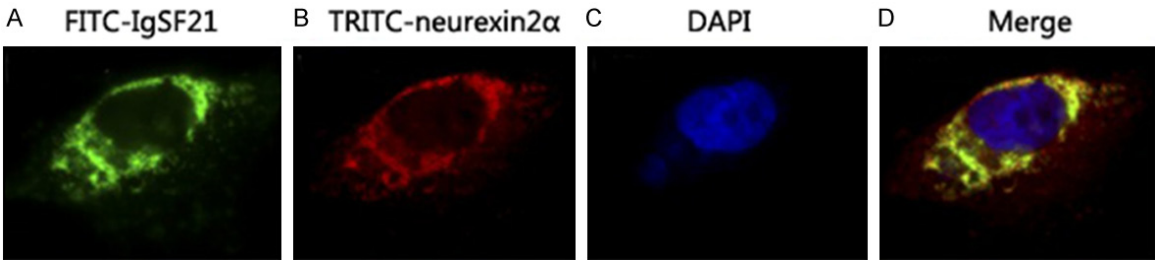

Figure 3. Spatial localization of IgSF21 and neurexin2α in cells. A: Spatial localization of IgSF21 in cell; B: Spatial localization of neurexin2α in cell; C: The nucleus was stained with DAPI; D: Image A and image B were merged (×600). IgSF21, immunoglobulin superfamily member 21; FITC, fluorescein isothiocyanate; TRITC, tetramethylrhodamine; DAPI, 4', 6-diamidino-2-phenylindole.

by centrifugation at 1,500 rpm for 10 minutes. Supernatant was discarded and sample was washed in PBS twice. Next, 1.5 mL pre-cooled radio-immunoprecipitation assay (RIPA) solution was added into the centrifuge tube and tube was placed on ice for 30 minutes. After centrifugation, the supernatant was transferred into Eppendorf tubes labeled No. 1 and No. 2. Anti-IgSF21 and anti-neurexin2α antibodies and immunoglobulin G (IgG) were added, according to the instruction manual. Following a 6-hour agitation, protein A/G was added and samples were being agitated again for 5 hours. After centrifugation, samples were rinsed in RIPA twice and placed in a water bath at 100°C. At the end, Western blot was performed to analyze the relative content of protein.

Effects of IgSF21 overexpression on mIPSCs in amacrine cells: GABAergic amacrine cells were extracted from normal rats for culture. Cells in logarithmic phase were selected and cell density was controlled at $5*10^5$/mL. Cells were placed in a 12-well plate (0.5 mL per well). DMEM was renewed one day before transfection. The transfection of pCMV-Myc-IgSF21 was performed according to the instruction manual of Lipofectamine-2000 and samples were incubated at 37°C for 72 hours in an atmosphere of 5% CO_2. Patch clamp technique was employed to measure effects of IgSF-21 overexpression on mIPSCs in amacrine cells.

Statistical analysis

SPSS 17.0 software was applied for statistical analysis. Measurement data are expressed as mean ± standard deviation. Comparison between two groups was conducted by independent-samples t test. Multiple groups were compared by one-way analysis of variance and Bonferroni post-hoc test. A value of $P<0.05$ was considered statistically significant.

Results

Changes in mIPSCs in GABAergic amacrine cells in rats with DR

By using the patch clamp technique, it was found that in comparison with control group, frequencies of mIPSCs in GABAergic amacrine cells in groups A, B and C all declined, with the extent of reduction being proportional to the course of DR ($P<0.05$). The current amplitude of mIPSCs in groups B and C also decreased ($P<0.05$). See **Figure 1**.

Expression of IgSF21 in amacrine cells

Compared with control group, IgSF21 mRNA expression in groups A, B, and C all declined ($P<0.05$) while the reduction in group C was the greatest ($P<0.05$). In addition, IgSF21 protein expression in groups B and C also decreased in comparison with control group ($P<0.05$). See **Figure 2**.

Co-localization of IgSF21 and neurexin2α in amacrine cells

Spatial localization of IgSF21 labeled with FITC (green fluorescence) and neurexin2α labeled with TRITC (red fluorescence) were observed through indirect IF. Expressions of the two proteins were found in both cell membrane system and cytoplasm. The merged image exhibited relatively strong yellow fluorescence, revealing that these two proteins were close to each other in space and co-localization may exist. See **Figure 3**.

Figure 4. Interaction between IgSF21 and neurexin2α. A: HA tag antibody immunoprecipitated HA-IgSF21, and Western blot detected Myc-neurexin2α (labeled with Myc); B: Myc tag antibody immunoprecipitated Myc-neurexin2α, and Western blot detected HA-IgSF21 (labeled with HA). IgSF21, immunoglobulin superfamily member 21.

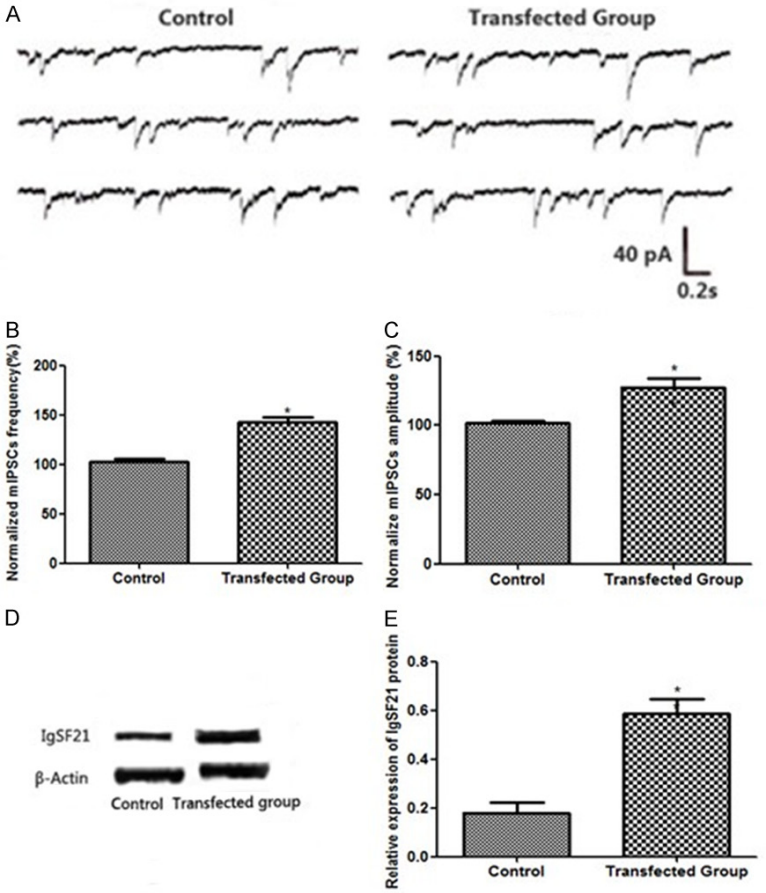

Figure 5. Effects of IgSF21 overexpression on mIPSCS in amacrine cells. A: Levels of mIPSCs in control and transfected groups measured by the patch clamp technique; B: Histogram of mIPSCs frequencies in control and transfected groups; C: Histogram of current amplitudes of mIPSCs in control and transfected groups; D: IgSF21 expression levels in the control and transfected groups; E: Histogram of IgSF21 expression levels in the control and transfected groups; *P<0.05 vs. control group. mIPCs, miniature inhibitory postsynaptic currents; IgSF21, immunoglobulin superfamily member 21.

Interaction between IgSF21 and neurexin2α tested by co-IP

Since co-localization of IgSF21 and neurexin2α in amacrine cells was detected by IF, co-IP was then conducted to check for any direct interaction between these two proteins. Co-transfection of pCMV-HA-IgSF21 plasmid labeled with HA and pCMV-Myc-neurexin-2α plasmid labeled with Myc was carried out and IgG was used as negative control. It was found that HA tag antibody could co-precipitate IgSF21 (labeled with HA) and Myc-neurexin2α was detected by Western blot, suggesting that neurexin2α could be precipitated by IgSF21. Meanwhile, Myc tag antibody could co-precipitate neurexin-2α (labeled with Myc) and HA-IgSF21 was detected by Western blot, indicating that IgSF21 could also be precipitated by neurexin2α. See **Figure 4**.

Effects of IgSF21 overexpression on mIPSCs in amacrine cells

The patch clamp test showed that in comparison with control, frequencies and current amplitudes of mIPSCs as well as levels of IgSF21 expression in GABAergic amacrine cells in the transfected groups all increased (all P<0.05). See **Figure 5**.

Discussion

Some studies have demonstrated that GABAergic amacrine cells are a type of inhibitory neuron and its malfunction induced by high blood sugar content can negatively affect neurotransmitter release and neurotransmission [10, 11]. In our study, we observed reduction in expressions of both IgSF21 gene and IgSF21 protein in amacrine cells from rats with DR, suggesting that the decrease in IgSF21 might be associated with progression of DR. There have been studies that have shown that mIPSCs in poultry can be suppressed when the function of their GABAergic amacrine cells is damaged, thus inducing occurrence of DR [12, 13]. By using the patch clamp technique, it was found that

both frequency and current amplitude of mIPSCs in GABAergic amacrine cells decreased to some extent, indicating some level of damage in retina amacrine cells. This result was consistent with previous findings [14].

Normal neurons can receive both excitatory glutamatergic inputs and inhibitory GABAergic inputs. Issues in either of these transmissions can interfere with neuron function [15, 16]. Neurexin2α is involved in regulating the L-type voltage-gated calcium channel that releases calcium ions out of cells and can activate and mediate PKC signaling pathways, change intracellular environment in retinal cells, and stimulate inhibitory GABAergic transmission. If activity of neurexin2α decreases, the function of GABAergic amacrine cells will be suppressed, further inducing DR [17]. In the present study, we performed IF and transfection and observed the spatial localization of IgSF21 and neurexin2α through indirect IF assay. We found expressions of these two proteins in both cell membrane system and cytoplasm. The merged image displayed relatively strong yellow fluorescence, demonstrating that the two proteins were close to each other in space. Therefore, our results suggest that IgSF21 may act on neurexin2α directly and impact its biological function. Mitchell et al. reported that ezrin factor can bind to neurexin2α, causing changes in mIPSCs of GABAergic amacrine cells in rats with DR [18, 19]. In order to further investigate the correlation between IgSF21 and neurexin2α, co-IP assay was conducted and direct interaction between these two proteins was found. Ting et al. reported that IgSF21 protein is related to DR, which aligns with our result [20]. However, the mechanism behind this has not been verified in their studies. Both the frequency and current amplitude of mIPSCs increased following overexpression of IgSF21 in amacrine cells ($P<0.05$), suggesting that IgSF21 can greatly affect mIPSCs, and is closely related to progression of DR.

In conclusion, high blood sugar content can induce reduction in IgSF21 levels while IgSF21 can adjust the function of GABAergic amacrine cells by interacting with neurexin2α. Our present study mainly investigated correlation between these two proteins. Effects of IgSF21 on signaling pathways have yet to be explored. Due to the complexity of DR pathogenesis, the mechanism of impact of high sugar content on IgSF21 levels was not studied this time. This requires further research in the future.

Disclosure of conflict of interest

None.

Address correspondence to: Xiaohui Lin, Department of Ophthalmology, The Inner Mongolia Autonomous Region People's Hospital, No. 20 Zhaowuda Road, Hohhot 010017, Inner Mongolia Autonomous Region, China. Tel: +86-15904895373; E-mail: xiaohuilin868@126.com

References

[1] Dodo Y, Murakami T, Suzuma K, Yoshitake S, Yoshitake T, Ishihara K, Fujimoto M, Miwa Y and Tsujikawa A. Diabetic neuroglial changes in the superficial and deep nonperfused areas on optical coherence tomography angiography. Invest Ophthalmol Vis Sci 2017; 58: 5870-5879.

[2] Nishikawa S, Kunikata H, Aizawa N and Nakazawa T. Bullous exudative retinal detachment after retinal pattern scan laser photocoagulation in diabetic retinopathy. Case Rep Ophthalmol 2017; 8: 475-481.

[3] Ratra D, Akhundova L and Das MK. Retinopathy of prematurity like retinopathy in full-term infants. Oman J Ophthalmol 2017; 10: 167-172.

[4] Shah AR, Yonekawa Y, Todorich B, Van Laere L, Hussain R, Woodward MA, Abbey AM and Wolfe JD. Prediction of anti-VEGF response in diabetic macular edema after 1 injection. J Vitreoretin Dis 2017; 1: 169-174.

[5] Park S, Rhee SY, Jeong SJ, Kim K, Chon S, Yu SY and Woo JT. Features of long-standing korean type 2 diabetes mellitus patients with diabetic retinopathy: a study based on standardized clinical data. Diabetes Metab J 2017; 41: 393-404.

[6] Boss JD, Singh PK, Pandya HK, Tosi J, Kim C, Tewari A, Juzych MS, Abrams GW and Kumar A. Assessment of neurotrophins and inflammatory mediators in vitreous of patients with diabetic retinopathy. Invest Ophthalmol Vis Sci 2017; 58: 5594-5603.

[7] Zhang X, Yang J, Zhong Y, Xu L, Wang O, Huang P, Li C, Qu B, Wang J, Zheng C, Niu M and Yu W. Association of bone metabolic markers with diabetic retinopathy and diabetic macular edema in elderly Chinese individuals with type 2 diabetes mellitus. Am J Med Sci 2017; 354: 355-361.

[8] Mastropasqua R, Toto L, Mastropasqua A, Aloia R, De Nicola C, Mattei PA, Di Marzio G, Di Nicola M and Di Antonio L. Foveal avascular

zone area and parafoveal vessel density measurements in different stages of diabetic retinopathy by optical coherence tomography angiography. Int J Ophthalmol 2017; 10: 1545-1551.

[9] Gella L, Raman R, Kulothungan V, Pal SS, Ganesan S, Srinivasan S and Sharma T. Color vision abnormalities in type II diabetes: sankara nethralaya diabetic retinopathy epidemiology and molecular genetics study II report no 2. Indian J Ophthalmol 2017; 65: 989-994.

[10] Yoshida S, Kobayashi Y, Nakao S, Sassa Y, Hisatomi T, Ikeda Y, Oshima Y, Kono T, Ishibashi T and Sonoda KH. Differential association of elevated inflammatory cytokines with postoperative fibrous proliferation and neovascularization after unsuccessful vitrectomy in eyes with proliferative diabetic retinopathy. Clin Ophthalmol 2017; 11: 1697-1705.

[11] Khalaf N, Helmy H, Labib H, Fahmy I, El Hamid MA and Moemen L. Role of angiopoietins and Tie-2 in diabetic retinopathy. Electron Physician 2017; 9: 5031-5035.

[12] Rho SS, Ando K and Fukuhara S. Dynamic regulation of vascular permeability by vascular endothelial cadherin-mediated endothelial cell-cell junctions. J Nippon Med Sch 2017; 84: 148-159.

[13] Van Katwyk S, Jin YP, Trope GE, Buys Y, Masucci L, Wedge R, Flanagan J, Brent MH, El-Defrawy S, Tu HA and Thavorn K. Cost-utility analysis of extending public health insurance coverage to include diabetic retinopathy screening by optometrists. Value Health 2017; 20: 1034-1040.

[14] Shao J, Yin Y, Yin X, Ji L, Xin Y, Zou J and Yao Y. Transthyretin exerts pro-apoptotic effects in human retinal microvascular endothelial cells through a GRP78-dependent pathway in diabetic retinopathy. Cell Physiol Biochem 2017; 43: 788-800.

[15] Korobelnik JF, Rougier MB and Delyfer MN. Wide field OCT-angiography of a patient with proliferative diabetic retinopathy. J Fr Ophtalmol 2017; 40: 721-722.

[16] Rezzola S, Nawaz IM, Cancarini A, Ravelli C, Calza S, Semeraro F and Presta M. 3D endothelial cell spheroid/human vitreous humor assay for the characterization of anti-angiogenic inhibitors for the treatment of proliferative diabetic retinopathy. Angiogenesis 2017; 20: 629-640.

[17] Wang Z, Camino A, Zhang M, Wang J, Hwang TS, Wilson DJ, Huang D, Li D and Jia Y. Automated detection of photoreceptor disruption in mild diabetic retinopathy on volumetric optical coherence tomography. Biomed Opt Express 2017; 8: 5384-5398.

[18] Mitchell SL, Neininger AC, Bruce CN, Chocron IM, Bregman JA, Estopinal CB, Muhammad A, Umfress AC, Jarrell KL, Warden C, Harlow PA, Wellons M, Samuels DC and Brantley MA Jr. Mitochondrial haplogroups modify the effect of diabetes duration and HbA1c on proliferative diabetic retinopathy risk in patients with type 2 diabetes. Invest Ophthalmol Vis Sci 2017; 58: 6481-6488.

[19] Fenwick EK, Khadka J, Pesudovs K, Rees G, Wong TY and Lamoureux EL. Diabetic retinopathy and macular edema quality-of-life item banks: development and initial evaluation using computerized adaptive testing. Invest Ophthalmol Vis Sci 2017; 58: 6379-6387.

[20] Ting DSW, Cheung CY, Lim G, Tan GSW, Quang ND, Gan A, Hamzah H, Garcia-Franco R, San Yeo IY, Lee SY, Wong EYM, Sabanayagam C, Baskaran M, Ibrahim F, Tan NC, Finkelstein EA, Lamoureux EL, Wong IY, Bressler NM, Sivaprasad S, Varma R, Jonas JB, He MG, Cheng CY, Cheung GCM, Aung T, Hsu W, Lee ML and Wong TY. Development and validation of a deep learning system for diabetic retinopathy and related eye diseases using retinal images from multiethnic populations with diabetes. JAMA 2017; 318: 2211-2223.